J Mol Model (2006) 12: 563–568
DOI 10.1007/s00894-005-0056-0

ORIGINAL PAPER

F. Matthias Bickelhaupt · Miquel Solà · Célia Fonseca Guerra

Structure and bonding of methyl alkali metal molecules

Received: 24 March 2005 / Accepted: 26 September 2005 / Published online: 13 January 2006

Abstract We have carried out a theoretical investigation of the methyl alkali metals CH_3M with M=Li, Na, K and Rb using density functional theory (DFT) at the BP86/TZ2P level. Our purpose is to determine how the structure and thermochemistry (e.g., C–M bond lengths and strengths) of these organoalkali metal compounds depend on the metal atom, and to understand the emerging trends in terms of quantitative Kohn–Sham molecular orbital (KS-MO) theory. The C–M bond becomes longer and *weaker* if one goes from Li to the more electropositive Rb. Also, the polarity of the C–M bond increases along this series but it preserves a strong intrinsic preference to homolytic over ionic dissociation in the gas phase. We show that a description of the bonding mechanism in terms of a polar C–M electron-pair bond between the methyl radical and alkali metal atom is just as natural as an ionic description (i.e., in terms of CH_3^-+M^+) and that it provides a straightforward way of understanding all observed trends.

Keywords Alkali metals · Bonding theory · Density functional calculations · Lithium · Polar bonds

Introduction

Organoalkali metal compounds, in particular organolithium reagents, are both archetypal and of practical importance: they constitute the simplest organometallic compounds and, at the same time, are widely used in organic synthesis [1]. Many studies have been directed towards unraveling the nature of these compounds. Early pioneering studies by the groups of Schleyer and Pople [2], Lipscomb [3], and Ahlrichs [4] highlighted the covalent aspects of the carbon–lithium bond (see Structure **1**), especially in organolithium aggregates. This view is also supported by the large carbon–lithium NMR coupling constants of up to 17 Hz observed for organolithium aggregates [5–8].

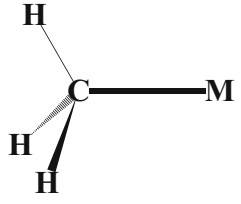

1

In contrast, Streitwieser and coworkers [9] were the first to emphasize the highly polar character of this bond based on a more advanced scheme for computing atomic charges, the integrated projected populations (IPP). This approach yields an atomic charge of Li in methyllithium of +0.8 a.u. Other studies have also been in support of a lithium atomic charge close to +1 a.u., for example, natural population analysis (NPA) [10, 11] and atoms in molecules (AIM) [12], which yield charges close to +0.9 a.u. In addition, Streitwieser, Bushby, and Steel have shown that a simple electrostatic model is able to reproduce the ratio of carbon–carbon and lithium–lithium distances in the methyl lithium tetramer [13–15]. These results have led to the current picture [16–25] of an 80–90% ionic C–Li bond that can best be understood in terms of a CH_3^- anion and a Li^+ cation in-

Dedicated to Professor Dr. Paul von Raqué Schleyer on the occasion of his 75th birthday

F. M. Bickelhaupt (✉) · C. Fonseca Guerra
Theoretische Chemie,
Scheikundig Laboratorium der Vrije Universiteit,
De Boelelaan 1083,
NL-1081HV Amsterdam, The Netherlands
e-mail: FM.Bickelhaupt@few.vu.nl
Fax: +31-20-5987629

M. Solà
Institut de Química Computacional and
Departament de Química,
Universitat de Girona,
Campus Montilivi,
E-17071 Girona, Catalonia, Spain

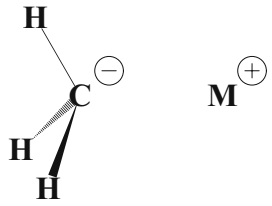

2

teracting predominantly electrostatically with only marginal covalent character (see Structure **2**).

The purpose of the present study is twofold. In the first place, we wish to augment the scarce structural and thermodynamic information on organoalkali metal compounds (vide infra) with a set of data that is obtained consistently at the same level of theory and, thus, to enable a systematic analysis of trends. Thus, we compute at the BP86/TZ2P level of density functional theory (DFT) [26] how the structure and thermochemistry (e.g., C–*M* bond lengths and strengths) of methyl alkali metal compounds CH_3M depend on the metal atom, along *M*=Li, Na, K and Rb. A second purpose is to understand the emerging trends in terms of quantitative Kohn–Sham molecular orbital (KS-MO) theory [27]. In particular, we show that a description of the bonding mechanism in terms of a polar C–*M* electron-pair bond between the methyl radical and alkali metal atom is just as natural as an ionic description (i.e., in terms of CH_3^-+M^+) and that it provides a straightforward way of understanding all observed trends. In the course of this work, we present a new implementation into our Amsterdam Density Functional (ADF) program [26] for computing Kohn–Sham Fock matrix elements in terms of fragment molecular orbitals (MOs).

Materials and methods

Computational details

All computations were carried out with the ADF program [26] at the BP86/TZ2P level of the generalized gradient approximation (GGA) of Kohn–Sham density functional theory (DFT) [27]. The TZ2P basis set consists of uncontracted set of Slater-type orbitals (STOs), including diffuse functions. It is of triple-ζ quality for all atoms and has been augmented with two sets of polarization functions: 3d and 4f on C, Li, Na; 4d and 4f on K, Rb; and 2p and 3d on H. In addition, an extra set of *p*-functions was added to the basis sets of Li (2p), Na (3p), K (4p) and Rb (5p). The 1s core shell of carbon and lithium, the 1s2s2p core shells of sodium and potassium, and the 1s2s3s2p3p3d core shells of rubidium were treated by the frozen-core (FC) approximation. An auxiliary set of s-, p-, d-, f- and g-STOs was used to fit the molecular density and to represent the Coulomb and exchange-correlation potentials accurately in each SCF cycle. For a more detailed description of our methods and the ADF program, see [26] and [27].

Fock matrix elements in terms of fragment MOs

The ADF program has the option to analyze the interaction energy between two molecular fragments by building up the molecule from these either mono- or polyatomic fragments. The molecular orbitals $\left\{\psi_j^\Gamma\right\}$ that are computed are then expressed as linear combinations of the symmetry-adapted fragment orbitals $\left\{\varphi_j^\Gamma\right\}$, i.e., symmetry-adapted linear combinations of the molecular orbitals *of the fragments under consideration*, which in turn can be written as linear combinations of STO basis functions $\{\chi_k\}$:

$$\psi_{\mathrm{i}}^\Gamma = \sum_{\mathrm{j}} a_{\mathrm{ij}}^\Gamma \varphi_{\mathrm{j}}^\Gamma = \sum_{\mathrm{k}} b_{\mathrm{ik}}^\Gamma \chi_k \tag{1}$$

For the Kohn–Sham Fock matrix $\mathbf{F}_{\mathrm{KS}}$ in the basis of the symmetry-adapted fragment orbitals, the generalized Eigenvalue problem holds, i.e.,

$$\mathbf{F}_{\mathrm{KS}}\mathbf{C} = \mathbf{S}\,\mathbf{C}\,\mathbf{E} \tag{2}$$

with the Kohn–Sham Fock matrix elements given by

$$(F_{KS})_{ij} = \left\langle \varphi_i^\Gamma \middle| \hat{F}_{KS} \middle| \varphi_J^\Gamma \right\rangle \tag{3}$$

The Kohn–Sham Fock matrix elements correspond the coupling or interaction strength between two orbitals φ_i^Γ and φ_j^Γ. They can be obtained either with the potential of the promolecule density (i.e., the initial sum of fragment densities) or with the final molecular density. The former case corresponds to the field that the orbitals are exposed to before they start interacting but after the fragments have adopted their positions in the overall molecule. In the latter case, solution of the generalized Eigenvalue problem of Eq. (2) yields the molecular Kohn–Sham orbitals ψ_i^Γ and orbital energies $\varepsilon_i = \left\langle \psi_i^\Gamma \middle| \hat{F}_{KS} \middle| \psi_i^\Gamma \right\rangle$. In the present study, we use the latter interaction matrix elements. We wish to point out, however, that the two choices yield similar values that show exactly the same trends.

Results and discussion

Structures and energies

The results of our BP86/TZ2P computations on methyl lithium, sodium, potassium and rubidium are collected in Table 1. Our computed homolytic bond dissociation enthalpies (BDE for 298 K) and bond lengths (see Table 1) agree within a few kcal mol^{-1} and a few hundredths of an angstrom (Å), respectively, with the available experimental [28] and/or with other DFT and ab initio results [10, 11, 16–25]. The computed strength (i.e., BDE) of the C–*M* bond in

Table 1 Analysis of the C–*M* bond between $CH_3^{\bullet}$ and $M^{\bullet}$ in CH_3M[a]

Property	CH_3Li	CH_3Na	CH_3K	CH_3Rb
Geometry (in Å, degree)				
C–*M*	2.010	2.376	2.747	2.821
C–H	1.105	1.098	1.100	1.096
H–C–H	106.48	109.84	109.14	109.63
Bond energy decomposition (in kcal mol^{-1})[b]				
ΔE_{oi}	−63.1	−42.2	−38.4	−42.2
ΔV_{elstat}	−30.3	−23.3	−19.0	−20.4
ΔE_{Pauli}	38.4	27.8	23.4	30.7
ΔE_{int}	−55.0	−37.7	−34.0	−31.9
ΔE_{prep}	10.2	6.7	7.4	6.9
ΔE	−44.8	−31.0	−26.6	−25.0
ΔH^{298}=−BDE	−44.0	−30.3	−26.2	−24.6
Miscellaneous bonding parameters[c]				
S_{bond}	0.31	0.28	0.21	0.19
F_{bond}	−70.3	−61.5	−40.2	d
$\varepsilon(ns)-\varepsilon(2a_1)$	3.2	3.4	3.8	4.0
Q(M)	0.386	0.351	0.428	0.466

[a]Computed at BP86/TZ2P
[b]$\Delta E=\Delta E_{prep}+\Delta E_{int}$; $\Delta E_{int}=\Delta V_{elstat}+\Delta E_{Pauli}+\Delta E_{oi}$ (see text)
[c]Interaction matrix elements between SOMOs F_{bond} in kcal mol^{-1}; bond overlap S_{bond}; orbital energy difference $\varepsilon(ns)-\varepsilon(2a_1)$ in eV; VDD atomic charges Q(M) in a.u
[d]Cannot yet be computed for Rb, for technical reasons

methyl alkali metal monomers decreases if one descends the periodic table, from 44.0 (Li) to 30.3 (Na) to 26.2 (K) to 24.6 kcal mol^{-1} (Rb). The computed C–*M* bond distances increase monotonically from 2.010 (Li) to 2.376 (Na) to 2.747 (K) to 2.821 Å (Rb), in agreement with mm-wave spectroscopy experiments of Grotjahn et al. for *M*=Li, Na and K [28, 29]. Note that our H–C–H angles are systematically smaller for CH_3Li (106.48°) than for the heavier homologous (109–110°), in line with CCSD(T) calculations [18] for CH_3Li and CH_3Na. The mm-wave experiments [28, 29], on the other hand, yield essentially constant M–C–H angles of 107.2, 107.3 and 107.0°, along the series Li, Na and K. Thus, for methyl rubidium, for which an experimental structure has not yet been published, we predict a C–*M* bond length that is about 0.07 Å longer than that in methyl potassium, whereas the methyl has essentially the same structure in both molecules.

Bonding mechanism

Our analyses of the C–*M* bond comprize three complementary approaches: (1) decomposition of the electronic bond energy ΔE; (2) quantitative analysis of the Kohn–Sham orbital electronic structure; (3) analysis of the electron-density distribution using various atomic charge schemes. The bond energy ΔE corresponds to the reaction $CH_3^{\bullet}+M^{\bullet}\rightarrow CH_3M$ and is first divided into the preparation energy ΔE_{prep} associated with deforming the methyl radical (from its planar equilibrium structure to the pyramidal geometry it adopts in CH_3M) and the actual interaction energy ΔE_{int} between pyramidal $CH_3^{\bullet}$ and $M^{\bullet}$ radicals. ΔE_{prep} is somewhat more destabilizing in methyl lithium than in the heavier homologues owing to the stronger C–Li interaction, which causes the above-mentioned higher extent of methyl pyramidalization in CH_3Li. The interaction energy ΔE_{int} shows the same trend as ΔE and ΔH^{298}: it weakens strongly from Li to Na and then more moderately along Na, K and Rb. We have further decomposed ΔE_{int} into the electrostatic attraction ΔV_{elstat} between the unperturbed charge distributions of the $CH_3^{\bullet}$ and $M^{\bullet}$ fragments, the Pauli repulsive orbital interaction ΔE_{Pauli} (between occupied orbitals) and the bonding orbital interactions ΔE_{oi} that are provided by electron-pair bonding and donor-acceptor interactions [27].

Interestingly, the more dominant of the two bonding terms is the orbital interactions ΔE_{oi} (which is between −63 and −38 kcal mol^{-1}) and not the electrostatic attraction ΔV_{elstat} (which is between −30 and −19 kcal mol^{-1}). This may be surprizing at first if one proceeds from the ionic model, in which the cohesion in the C–*M* bond is ascribed to electrostatic attraction between CH_3^- and M^+ ions in a nearly salt-like, ionic CH_3M. Note, however, that, electrostatically, the charge separation across the C–*M* bond is energetically unfavorable in the gas-phase compared to a more balanced (less polar) charge distribution.

Of course, this changes in solution as the solvent molecules interact strongly with, and thus stabilize, the ionic fragments of the heterolytic dissociation pathway. Note however that in solution, a physically correct description of a methyl alkali metal consequently involves (at least) a few solvent molecules of the first solvation shell and that the system is rather to be conceived as a methyl alkali metal–solvent complex. Here, we focus our analysis to the intrinsic nature of carbon–metal bonding as it exists, unaffected by solvent molecules, in the gas phase.

However, also in the gas phase, charge separation still occurs because of the electronegativity difference between $CH_3^{\bullet}$ and M$^{\bullet}$, that is, the fact that the energy of the $2a_1$ singly occupied molecular orbital (SOMO) on the $CH_3^{\bullet}$ radical is significantly lower than that of the *ns* SOMO on the M$^{\bullet}$ atom (see orbital energy differences $\varepsilon(ns)$-$\varepsilon(2a_1)$ in Table 1). This is nicely illustrated by examining the heterolytic dissociation of CH_3M into CH_3^-+M$^+$ (values not shown in Table 1). Here, the electrostatic interaction dominates by far: ΔV_{elstat} is between −197 (Li) and −158 kcal mol^{-1} (K) whereas ΔE_{oi} is only between −21 (Li) and −18 kcal mol^{-1} (K). In CH_3Li, for example, the heterolytic bond energy ΔE_{hetero} between CH_3^-+M$^+$ amounts to −174.2 kcal mol^{-1}, which arises from −197.4 kcal mol^{-1} of electrostatic attraction ΔV_{elstat}, −21.1 kcal mol^{-1} of orbital interactions ΔE_{oi} and 44.0 kcal mol^{-1} of Pauli repulsion. The weakening of the electrostatic interaction in the heterolytic dissociation on going from Li to Rb is due to the increase in the *M*–C bond length, which is not compensated by the smaller charge transfer from CH_3^- to M$^+$ along the Li–Rb series. However, the heterolytic process is much more endothermic (−ΔE-

hetero=175–124 kcal mol^{-1}) than homolytic dissociation ($-\Delta E$=45–25 kcal mol^{-1}) because of the ionization energy that must be invested to remove an electron from M$^{\cdot}$ and transfer it to $CH_3^{\cdot}$. It is of course perfectly valid to compute the homolytic bond energy in two steps by adding the reaction energies of $CH_3^{\cdot}+M^{\cdot}\rightarrow CH_3^- + M^+$ (charge separation) and $CH_3^- + M^+ \rightarrow CH_3M$ (heterolytic bond formation) [30]. However, ΔE_{hetero} alone provides only incomplete information about the quantity we are actually interested in, i.e., the homolytic bond strength ΔE in the gas phase. Moreover, we feel that analyzing the homolytic bond energy ΔE, i.e., the reaction energy for $CH_3^{\cdot}+M^{\cdot}\rightarrow CH_3M$, directly in terms of the bonding between the corresponding neutral molecular fragments provides a more straightforward description and understanding of its origin and of trends therein, than first analyzing the bonding between the ionic fragments CH_3^- and M^+, associated with a different, energetically (ΔE_{hetero}) much disfavored ionic dissociation, and adding the charge-transfer energy also to obtain ΔE. On the other hand, the origin in the heterolytic bond energy ΔE_{hetero}, i.e. the reaction energy for $CH_3^- + M^+ \rightarrow CH_3M$, is obviously most directly described in terms of the interaction between the methyl anion and alkali metal cation, which indeed is predominantly electrostatic (vide supra).

Both, electrostatic attraction ΔV_{elstat} and Pauli repulsion ΔE_{Pauli} between $CH_3^{\cdot}$ and $M^{\cdot}$ become weaker along Li–K. The common origin of these trends, which partially cancel each other, is the decreasing overlap between occupied orbitals of $CH_3^{\cdot}$ and $M^{\cdot}$ as the metal AOs become more extended and diffuse. The dominant contributor to the trend in ΔE is the orbital interaction ΔE_{oi}, which (just as ΔV_{elstat}) weakens along Li–K from −63.1 to −42.2 to −38.4 kcal mol^{-1}. The trend in ΔE_{oi} and, thus, in the thermodynamic stability ΔE (or ΔH^{298}=−BDE) can be traced directly to covalent features in the bonding mechanism, i.e., the bond overlap between and mixing of the SOMOs that yield the electron-pair bond. Our quantitative analyses of the orbital electronic structure show that this electron-pair bonding $2a_1$+*ns* combination between the methyl and alkali metal SOMOs is polarized toward methyl. However, they also reveal that the alkali metal *ns* contribution is not at all marginal: in terms of Gross Mulliken contributions [31] the composition is approximately 70% $2a_1$+25% *ns*. In case of methyl lithium, the situation is 70% $2a_1$+24% 2s with, in addition, a sizeable contribution of 7% from the lithium $2p_\sigma$ AO. In terms of mixing coefficients [31], this is $0.72\,2a_1 + 0.53\,2s\,(+0.32\,2p_\sigma)$. We recall that the stabilization of the bonding $2a_1$+*ns* combination relative to $\varepsilon(2a_1)$, i.e., the covalent contribution to the orbital interactions ΔE_{oi}, is to second order equal to $F_{bond}^2/\varepsilon(2a_1)-\varepsilon(ns)$, that is, the interaction matrix element $F_{bond} = \langle 2a_1 \left| \hat{F} \right| ns \rangle$ squared and divided by the difference in orbital energies and that F_{bond} is in good approximation proportional to the bond overlap $S_{bond} = \langle 2a_1 | ns \rangle$ [32], as illustrated by **3**.

The bond overlap S_{bond} is sizeable and decreases from 0.31 to 0.28 to 0.21 to 0.19 along *M*=Li, Na, K and Rb. This is because the metal *ns* AOs become more diffuse and extended along this series, which causes the optimum overlap to become smaller and to be achieved at longer bond distances [33]. The corresponding interaction-matrix elements F_{bond} show the same trend as S_{bond}; they are sizeable and weaken from −70.3 to −61.5 to −40.2 kcal mol^{-1} along Li, Na and K (see Table 1). This leads to the observed weakening of ΔE_{oi} along Li–K [34], as illustrated by **3**→**4**, and contributes significantly to the same trend in the overall C-M bond strength. The loss of ΔE_{oi} is largest from Li to Na because, in addition to the decreasing bond overlap, the stabilizing admixture of the low-energy lithium $2p_\sigma$ AO into the electron-pair bonding combination is lost.

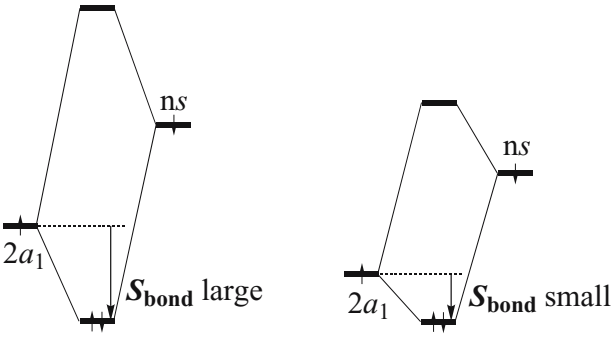

3 **4**

Note that ionic bonding would have led to the opposite trend in ΔE_{oi}, that is, an increase of the orbital interactions along Li–Rb. To understand this, we must first realize that ionic bonding between $CH_3^{\cdot}$ and $M^{\cdot}$ radicals corresponds, in terms of orbital interactions, to the complete transfer of an electron from the metal *ns* to the methyl $2a_1$ orbital and the absence of mixing between these SOMOs. This is illustrated schematically below in **5**.

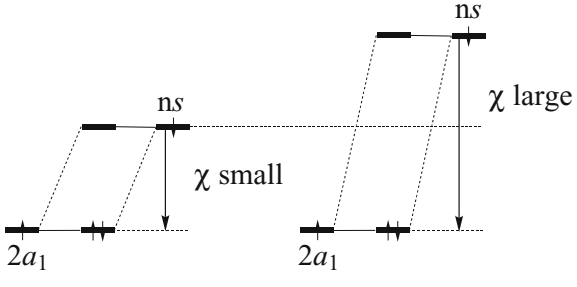

5 **6**

The electron of the metal drops, so to say, into the methyl $2a_1$ (which becomes a lone-pair like MO) and the orbital interactions ΔE_{oi} now originate from the associated orbital energy difference $\varepsilon(2a_1)$–$\varepsilon(ns)$. The latter, which can also be associated with the difference in electronegativity $\Delta\chi$ [35], increases along Li–Rb and so should ΔE_{oi} (see **5**→**6**) if the ionic aspect were to dominate the trend in the $CH_3^{\cdot}+M^{\cdot}\rightarrow CH_3M$ process. This is apparently not what happens.

Alkali metal atomic charges

The above description of the C–M bond (see **3** and **4**) as an electron-pair bond with significant covalent character (i.e., stabilization through bond overlap) is not at all in contradiction with a high polarity. Indeed, we find a wave function (electron-pair bonding MO) that is polarized toward carbon, and our Li atomic charge is +0.89, +0.50 and +0.39 a.u. according to the atoms in molecules (AIM), Hirshfeld and Voronoi deformation density (VDD) methods (see Table 1 for VDD charges Q(M) along Li–Rb) [10, 36]. The VDD atomic charge appears to be very close to the GAPT (generalized atomic polar tensors) charge of +0.4178 a.u. computed by Cioslowski at the HF/6-31G** level [37]. The polarity across the C–*M* bond arises of course from the difference in energy of the SOMOs of the methyl radical and the lithium atom (i.e., the electronegativity difference $\Delta\chi$). As pointed out in the introduction, the current ionic picture of the C–Li bond is based to an important extent on this polarization, in particular, on the atomic charge of Li in methyl lithium that in earlier studies was mostly found being close to +1 a.u. (i.e., +0.8, +0.85 and +0.9 a.u. according to IPP [9], NPA [10], and AIM [12] methods). This was interpreted as indicating that the C–Li bond is 80–90% ionic. The present study confirms that the C–Li bond is highly polar. However, as has been pointed out recently [36], atomic charges are not absolute bond-polarity indicators. Different atomic charge methods have different scales: the atomic charge of exactly the same atom in exactly the same chemical environment may differ dramatically from one method to another (e.g. Li in CH_3Li is +0.89 a.u. and +0.39 a.u. according to AIM and VDD). Atomic charges become meaningful only through the comparison of trends in values computed with the same method. Thus, one can conclude that all atomic-charge schemes indicate that the C–*M* bond is significantly more polar than most other bonds [36]. Furthermore, a high polarity does not rule out a prominent role for a stabilization of the C–*M* electron-pair bonding MO due to bond overlap between the SOMOs of the $CH_3^{\bullet}$ and $M^{\bullet}$ radicals. In fact, as illustrated in **3** and **4**, "covalent" and "ionic" stabilization (i.e., stabilization caused by bond overlap and electronegativity difference, respectively) occur in general simultaneously in polar bonds. In the case of the C–*M* bond in CH_3M, the trend of the *decreasing* bond overlap S_{bond} along *M*=Li, Na, K and Rb overrules the trend of the *increasing* electronegativity difference $\Delta\chi$, which derives from the difference in SOMO energies $\varepsilon(ns)-\varepsilon(2a_1)$ (see table 1). This is not because the electronegativity difference is small but because it changes relatively little compared to changes in the stabilization due to S_{bond}.

Conclusions

The C–*M* bond in methyl alkali metal systems becomes longer and *weaker* if one goes from Li to the more electropositive Rb as follows from our BP86/TZ2P computations. For methyl rubidium, the structure of which has not yet been characterized experimentally, we predict a C–*M* bond length of 2.821 Å, that is, about 0.07 Å longer than that in methyl potassium, whereas the methyl has essentially the same structure in both molecules. Also, the polarity of the C–*M* bond increases along Li–Rb but it preserves a strong intrinsic preference to homolytic over ionic dissociation.

We have shown that a description of the bonding mechanism in terms of a polar C–*M* electron-pair bond between the methyl radical and alkali metal atom is just as natural as an ionic description (i.e., in terms of $CH_3^-+M^+$). In this picture, the weakening of the C–M bond along Li–Rb is ascribed to the decreasing bond overlap between the SOMOs of the $CH_3^{\bullet}+M^{\bullet}$ radicals into which this bond preferentially dissociates. This is not in contradiction with the fact that the C–M bond is highly polar.

Acknowledgements We thank the following organizations for financial support: HPC-Europa, the Deutsche Akademische Austauschdienst (DAAD), the National Research School Combination-Catalysis (NRSC-C), the Netherlands Organization for Scientific Research (NWO), the Ministerio de Educación y Cultura (MEC), the Training and Mobility of Researchers (TMR) program of the European Union, the Dirección General de Enseñanza Superior e Investigación Científica y Técnica (MEC-Spain) and the DURSI (Generalitat de Catalunya). Excellent service by the Stichting Academisch Rekencentrum Amsterdam (SARA) and the Centre de Supercomputació de Catalunya (CESCA) is gratefully acknowledged.

References

1. Elschenbroich C, Salzer A (1992) Organometallics. A concise indroduction, 2nd edn. VCH, Weinheim, Germany
2. Dill JD, Schleyer PR, Binckley JS, Pople JA (1977) J Am Chem Soc 99:6159–6173
3. Graham GD, Marynick DS, Lipscomb WN (1980) J Am Chem Soc 102:4572–4578
4. Schiffer H, Ahlrichs R (1986) Chem Phys Lett 124:172–176
5. Günther H, Moskau D, Bast P, Schmalz D (1987) Angew Chem, Int Ed Engl 26:1212–1220
6. Bauer W, Schleyer PR (1992) Adv Carbanion Chem 1:89–175
7. Bauer W (1995) Lithium Chemistry. Wiley-Interscience, New York
8. Fraenkel G, Martin KV (1995) J Am Chem Soc 117:10336–10344
9. Streitwieser A, Williams JE, Alexandratos S, McKelvey JM (1976) J Am Chem Soc 98:4778–4783
10. Bickelhaupt FM, van Eikema Hommes NJR, Fonseca Guerra C, Baerends EJ (1996) Organometallics 15:2923–2931
11. Lambert C, Kaupp M, Schleyer PvR (1993) Organometallics 12:853–859
12. Wiberg KB, Rablen PR (1993) J Comput Chem 14:1504–1518
13. Streitwieser Jr A (1978) J Organometal Chem 156:1–3
14. Bushby RJ, Steel HL (1987) J Organometal Chem 336:C25–C32
15. Bushby RJ, Steel HL (1990) J Chem Soc, Perkin Trans 2:1143–1153
16. Kwon O, Sevin F, McKee ML (2001) J Phys Chem A 105:913–922
17. Breidung J, Thiel W (2001) J Molec Struct 599:239–254
18. Scalmani G, Brédas JL (2000) J Chem Phys 112:1178–1191
19. Fressigné C, Maddaluno J, Giessner-Prettre C (1999) J Chem Soc, Perkin Trans 2:2197–2201
20. Kremer T, Harder S, Junge M, Schleyer PvR (1996) Organometallics 15:585–595

21. Tyerman SC, Corlett GK, Ellis AM, Claxton TA (1996) J Molec Struct (Theochem) 364:107–119
22. Lambert C, Schleyer PvR (1994) Angew Chem 106:1187–1199; Angew Chem Int Ed Engl 33:1129–1140
23. Wiberg K, Breneman CM (1990) J Am Chem Soc 112:8765–8775
24. Kaufmann E, Raghavachari K, Reed AE, Schleyer PvR (1988) Organometallics 7:1597–1607
25. Bauer W, Winchester WR, Schleyer PvR (1987) Organometallics 6:2371–2379
26. te Velde G, Bickelhaupt FM, Baerends EJ, van Gisbergen SJA, Fonseca Guerra C, Snijders JG, Ziegler T (2001) J Comput Chem 22:931–967
27. Bickelhaupt FM, Baerends EJ (2000) In: Lipkowitz KB, Boyd DB (eds) Reviews in computational chemistry, vol. 15. Wiley-VCH, New York p 1–86
28. Grotjahn DB, Pesch TC, Brewster MA, Ziurys LM (2000) J Am Chem Soc 122:4735–4741
29. Grotjahn DB, Pesch TC, Xin J, Ziurys LM (1997) J Am Chem Soc 119:12368–12369
30. Schmid R (2003) J Chem Ed 80:931–937
31. The description of the MO in terms of fragment MO *coefficients* in stead of Gross Mulliken contributions yields the same picture but it has the disadvantage of not being normalized, that is, the figures do not add up to 1 (or to 100%)
32. Albright TA, Burdet JK, Whangbo M-H (1985) Orbital interactions in chemistry. Wiley-Interscience, New York
33. The C-M bond distance also increases along Li–Rb because of the increasing number of metal core shells that enter into Pauli repulsion with closed shells on the methyl fragment. For a detailed discussion of how Pauli repulsion affects bond distances, see: Bickelhaupt FM, DeKock RL, Baerends EJ (2002) J Am Chem Soc 124:1500–1505
34. More subtle effects begin to play a role from K to Rb as the covalent character of the bond, and especially changes therein, become smaller
35. Mann JB, Meek TL, Knight ET, Capitani JF, Allen LC (2000) J Am Chem Soc 122:5132–5137
36. Fonseca Guerra C, Handgraaf J-W, Baerends EJ, Bickelhaupt FM (2004) J Comput Chem 25:189–210
37. Cioslowski J (1989) J Am Chem Soc 111:8333–8336